Study of the Influence of Phase Composition and Iron Content on the Formability Characteristics of Zinc-Iron Electroplated Sheet Steel

K. De Wit , A. De Boeck, and B.C. De Cooman

(Submitted 19 October 1998; in revised form 7 June 1999)

This study focuses on the relationship between coating composition and deformation and friction behavior of zinc-iron electroplated sheet steel. The influence of phase composition and microhardness of the deposits and the electrodeposition process parameters on the mechanical properties of the material were determined. The influence of coating composition on the friction and galling behavior was also investigated. Both V-bend test and cup test were used to evaluate the influence of the iron content on the powdering and flaking behavior of the deposits. Finally, the adhesion of the coating to the substrate was studied by lap shear tests.

Although the soft η phase appears to be the main component in zinc-iron coatings with less than 16 wt% Fe, Γ_1 particles were observed even at low iron contents. As the iron content in the coating increases, the Γ_1 fraction increases and the coating becomes harder and more brittle. Above 16 wt% Fe the deposits start to show substantial powdering and flaking during deformation. At iron contents above 30 wt%, bending of the coated product results in total coating delamination. At low iron contents, zinc-iron electroplated sheet steel exhibits a superior deformation behavior, and both cup tests and flat die tests proved the suitability of the coating for deep drawing.

Keywords coatings, electroplated coatings, friction, tribology, wear, zinc-iron coatings

1. Introduction

Zinc-iron alloy coated steel, such as galvannealed, is increasingly being used in the automotive industry due to its excellent corrosion resistance, weldability, and paintability (Ref 1-4). However, the deformation behavior of galvannealed steel remains an area of concern because the layered structure of intermetallic compounds has proved to be sensitive to powdering and adhesion loss (Ref 5-7).

A significant improvement of the powdering behavior can be expected when using zinc-iron electroplated coatings because they consist of homogeneous solid solutions (Ref 8, 9). Furthermore, because the electroplating process does not involve heating or cold working, it is expected that, in contrast with galvannealed steel, the mechanical properties of the base metal will not deteriorate as a result of the coating process.

A review of literature, however, shows that little information is available about the relationship between coating composition and deformation and friction behavior of zinc-iron electroplated sheet steel. A recent study by Liu (Ref 10) stated that in order to optimize the forming behavior of zinc-iron electrocoated material, the iron concentration should be chosen so that both powdering and friction coefficient are low during forming. Other sources report an excellent performance of the zinc-iron deposits with an iron content below 15 to 25 wt% Fe and poor workability at higher iron levels (Ref 3, 11, 12).

K. De Wit and **B.C. De Cooman,** Laboratory for Steelmaking, University of Ghent, Ghent, Belgium; and **A. De Boeck,** OCAS N.V., Research Center of the SIDMAR Group, Flat Rolled Products Division of ARBED, Zelzate, Belgium. Contact e-mail: katrien.dewit@rug.ac.be.

In this article, the results of an in-depth study on the relationship between the coating microstructure and the materials performance is reported. The phase composition and microhardness of the deposits, as well as the influence of the electrodeposition process on the mechanical properties of the material were determined. The influence of coating composition on the friction and galling behavior was also investigated, and both V-bend and cup tests were used to evaluate the influence of the iron content on the powdering and flaking behavior of the deposits. Finally, the adhesion of the coating to the substrate was studied by lap shear tests.

2. Experimental Procedure

The zinc-iron deposits were produced on a laboratory electroplating line using a sulfuric acid-based electrolyte consisting mainly of zinc sulfate and ferrous sulfate. Plating conditions such as iron/zinc ratio and current density were varied to obtain a wide range of coating compositions.

The composition of the deposited layers was determined by dissolving the coating in diluted HCl (Ref 13) and subsequent inductively coupled plasma (ICP) analysis of the solution. The phase composition and crystallographic texture were determined by x-ray diffraction using a Siemens D5000 diffractometer (Bruker Spectrospin, Brussels, Belgium) equipped with a copper tube. 2θ scans were performed between 30 and 90°. The hardness of the layers was measured with a Micro Duromat 4000 E microhardness tester (Reichert Jung) (Leica Microsystems AG, Wezlar, Germany). The mechanical properties of the coated and uncoated material were compared by a tensile test carried out on a MTS 810 testing machine (MTS, Berlin, Germany).

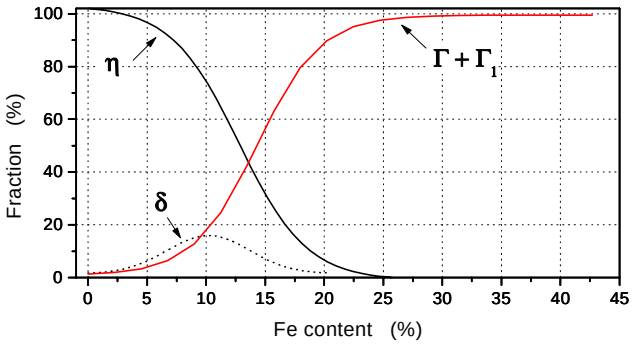

Fig. 2 Influence of the iron content on the phase distribution in electroplated zinc-iron coatings

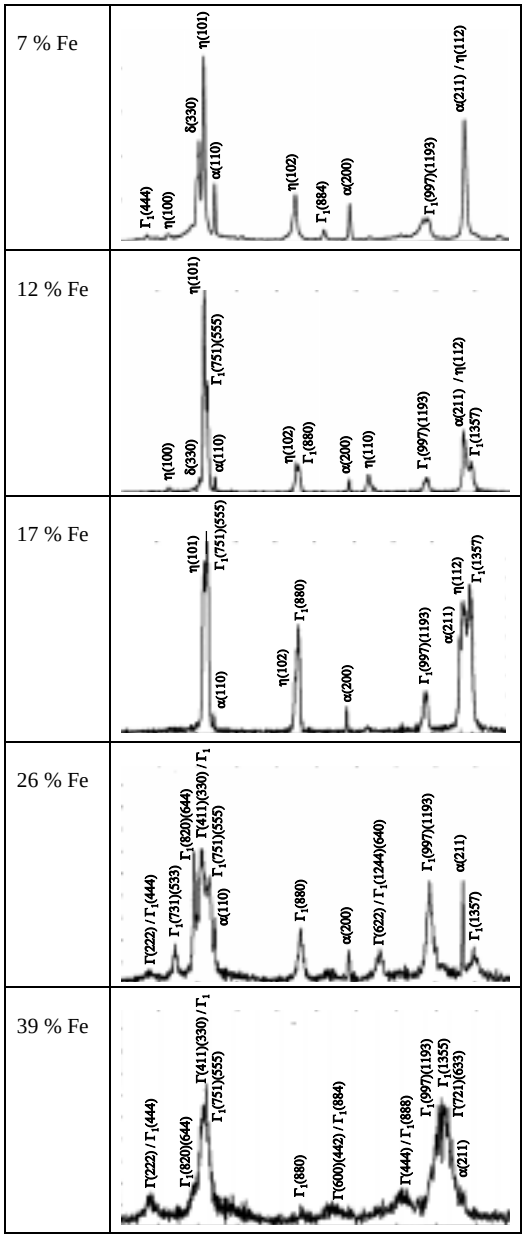

Fig. 1 Influence of the iron content on the phase composition of the coating

A first evaluation of the friction behavior of the as-deposited layers was performed on a SRV Tribometer (Optimol Instruments AG, Munchen, Germany; Ref 14). The sample was submitted to a horizontal oscillating movement while making contact with a flat die subjected to an increasing vertical load. The friction coefficient, *f*, was equal to the ratio, *T/N*, where *T* was the horizontal friction force and *N* was the applied vertical load. It was measured continuously in function of the load, which increased linearly from 0.5 to 2 MPa in 15 min. The samples were lubricated with the Quaker N6130 prelube oil (Quaker). The die material was a cast iron GG25, of which the contact surface had a controlled roughness with a R_a value between 0.3 and 0.4 μm, measured at cut-off length, λ_c, of 0.8 mm. The amount of galling was verified by three-dimensional measurements on the used tools.

Additional flat die tests were conducted to evaluate the friction behavior of the material. Strips, coated on both sides, were pulled between two flat jaws at a constant pressure of 5000 N and a drawing speed of 20 mm/min. The length of the stroke was 55 mm, and each sample passed ten times between the jaws. All samples were oiled before the first pass, and the subsequent passes were performed without additional oiling. After each pass, tools and steel strip were checked for the presence of galling. During the tests, pulling force and normal pressure were registered for function of sliding length, and the friction coefficient was calculated as the pulling force divided by twice the normal force.

The powdering and flaking behavior were studied by a 60° V-bend test and cup tests. The 60° V-bend test has the advantage of evaluating the resistance against delamination in bending-unbending without frictional effects (Ref 15-17), while the cup test is a closer simulation of the deep drawing process (Ref 18-19). Table 1 summarizes the cup test conditions. The formability of the zinc-iron coatings was evaluated by the weight loss after deformation. Weight loss expressed in g/m^2 was measured as the mean value of 20 individual measurements. The weight loss refers to the surface of the sample under the blankholder because the material under the punch does not participate in the deformation and is not damaged. The coatings were further examined using scanning electron microscopy using a Zeiss DSM 962 (Zeiss Inc.).

Finally, the adhesion between coating and substrate and the interfacial strength of the deposited layers were evaluated by a lap shear test (Ref 19, 20). In this test a single lap joint was exposed to tension in the direction of the bonding surface at a continuous speed until fracture. The lap shear strength is the load necessary to produce fracture divided by the surface area of the joint.

Table 1 Overview of the cup test conditions

Test conditions	Value
Blank diameter, mm	60
Punch diameter, mm	33
Blankholder force, kN	10
Drawing ratio	2
Drawing speed, m/s	600
Complete cups (no flange)	…
Cleaning of the die after each part	…

3. Results and Discussion

3.1 Phase Composition of the As-Deposited Zinc-Iron Layers

By changing the parameters of the electrodeposition process it was possible to obtain iron contents in the coatings ranging from 7 to 45 wt% (Ref 9). The coatings were examined using x-ray diffraction (XRD) to identify the crystal structure of the as-deposited layers. Figure 1 shows the XRD patterns for coatings with various iron contents. As is the case for galvannealed layers, zinc-iron electrodeposited coatings consist of a number of intermetallic compounds. However, whereas the different phases appear as stratified sublayers in a galvannealed coating, a more uniform distribution of the phases in the coating is obtained by electrodeposition (Ref 9). The identification of the different intermetallic phases is rather complicated due to the numerous overlaps of the single phase spectra and shifts of the peak positions due to lattice distortion (Ref 21, 22). Therefore, the peak identification was based on the interplanar spacings and resulting lattice constants. Figure 2 shows the phase distribution of the electrodeposited layers as a function of iron content.

The XRD profiles show the presence of the η phase in deposits with an iron content ranging from 7 to 22 wt%. The mean lines result from the low index pyramidal plane orientations $\eta(101)$ and $\eta(112)$ and from the prismatic $\eta(110)$ planes. Basal $\eta(002)$ reflections are absent. The *c/a* ratio is close to 1.60 for all samples, and no change in lattice constants in function of the iron content is seen in the observed range. Besides η, a small amount of δ and Γ/Γ_1 is present in the coatings. The δ phase reflections usually show very low intensities. As the iron content in the coating increases, the Γ/Γ_1 phase grows at the expense of η. The latter can be related to previous research findings where the interplanar spacings show a composition dependence for iron contents below 10 wt% (Ref 22, 23). Above 10 wt% Fe, the *c/a* ratio approaches the ideal value for hexagonal close packed structures. A further increase in iron content does not induce any change in lattice parameters because further distorsion of the lattice would raise the energy of the system. Thus the excess iron will lead to the formation of a second phase. As the iron content of the deposit increases, the amount of Γ/Γ_1 phase will increase. Figure 3 illustrates this change in crystal structure.

Above 16 wt% Fe, no η was present and Γ/Γ_1 was the principal phase. Because of the correlation between the Γ and the Γ_1 phase (Ref 24) an unambiguous identification of these phases is not possible. The presence of the Γ_1 phase was confirmed by reflections characteristic for a cubic face centered structure. However the extent of the Γ and Γ_1 fractions cannot be assessed.

3.2 Influence of the Coating Layer on the Mechanical Properties

Table 2 gives a comparison of the mechanical properties of the sheet steel before and after removal of the coating. The values indicated are mean values of three measurements. The results show that for a 10% Fe coating, electrodeposition has no influence on the mechanical properties. Due to the presence of a harder coating layer, a slight decrease in anisotropy coefficient and total elongation can be observed. However, in contrast with the changes reported for galvannealed and ZnNi coated sheet steel, this change should not be regarded as significant (Ref 25, 26). According to Liu (Ref 10), a significant deterioration of the *r*- and *n*-value of zinc-iron electroplated sheet steel might occur at higher iron contents or coating thicknesses.

3.3 Microhardness and Friction Coefficient of the As-Deposited Layers

Figure 4 shows the increase in microhardness of the as-deposited zinc-iron layers with increasing iron content. At low iron contents, where η is the main phase (<16 wt% Fe), zinc-iron electroplated layers have a higher microhardness than pure zinc coatings, but the microhardness stays significantly below that of galvannealed or electroplated zinc-nickel coatings. As the Γ_1 and Γ fraction in the coating increases, there

Table 2 Influence of an electrodeposited zinc-iron layer on the mechanical properties of the sheet steel

Material	Yield strength, MPa	Tensile strength, MPa	Uniform elongation, %	Total elongation, %	Anisotropy coefficient, $r_{0°}$	Strain hardening exponent, *n*
ZnFe coated (10% Fe-65 g/m^2)	208	341	23	37	1.22	0.217
Without coating	210	341	24	40	1.32	0.215

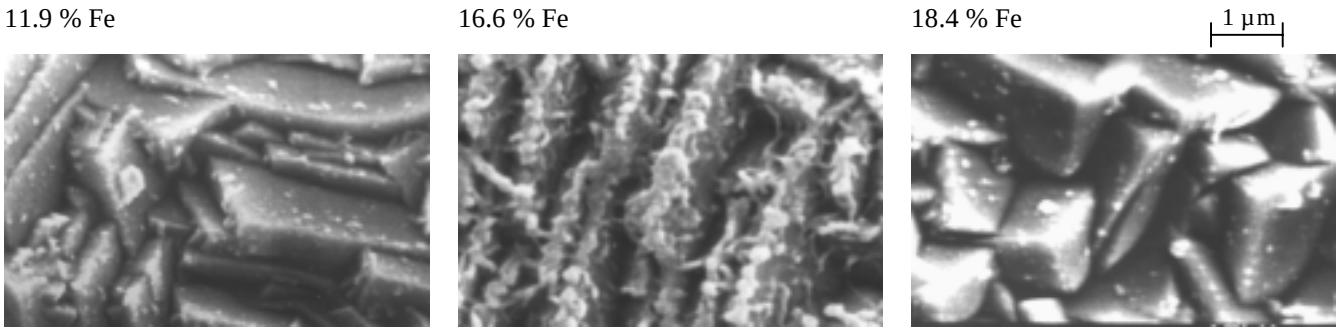

Fig. 3 Influence of the iron content on the surface morphology of electroplated zinc-iron coatings

is a significant increase in microhardness. The microhardness reaches the level of galvannealed and ZnNi layers at 40 wt% Fe.

A modified SRV Optimol test was carried out to evaluate the friction behavior of zinc-iron electrocoated materials. Figure 5 shows that contrary to galvannealed layers (Ref 27, 28) the amount of iron in the coating has no significant influence on the friction coefficient. This confirms the results previously obtained by Imlau (Ref 29) and Liu (Ref 10). Figure 5 also shows the difference in friction coefficient at the beginning (0.5 MPa) and at the end (2 MPa) of the tests. For the individual plots of the friction coefficient in load function it can be seen that at low normal pressures (0.5 to 0.6 MPa) a higher threshold value is obtained for zinc-iron coatings with low iron content. This is due to the presence of the soft η phase, which is prone to cold weld to the die material. At higher iron contents (>20 wt%) where all η has disappeared and Γ is present next to Γ_1, the fluctuations in the value of *f* are smaller. Visual evaluation of the tools revealed no galling. This was confirmed by three-dimensional profile analysis of the surface of a number of dies after the friction test.

Figure 6 summarizes the results of the flat die tests. The friction coefficient was determined at the end of the sliding distance of 50 mm for all passes to compare various materials with a uniform and reproducible criterion. The values indicated in Fig. 6 are all mean values of three tested samples. The results show that electroplated zinc-iron coatings have a lower friction coefficient compared to galvannealed coatings. Moreover, as the iron content of the layer increases from 8 to 14 wt%, the friction behavior becomes more stable and no stick slip occurs during the subsequent passes. This is due to the increasing amount of Γ and Γ_1 in the coating.

3.4 *Formability and Adhesion Characteristics of the Coatings*

A first evaluation of the powdering and flaking behavior of the electroplated layers was completed using a 60° V-bend test. Figure 7 shows the relationship between the amount of iron and the weight loss of the coating. Below 15 wt% Fe, the average coating weight loss is 0.35 mg. This shows that the performance of electroplated zinc-iron layers is considerably better than that of galvannealed coatings. At 15 wt% Fe the coating weight loss for galvannealed can increase to 4 mg (Ref 27). Above 15 wt% Fe, adhesion loss will increase significantly, and at 30 wt% Fe, weight losses of 10 mg and greater were measured. This increase in coating weight loss indicates

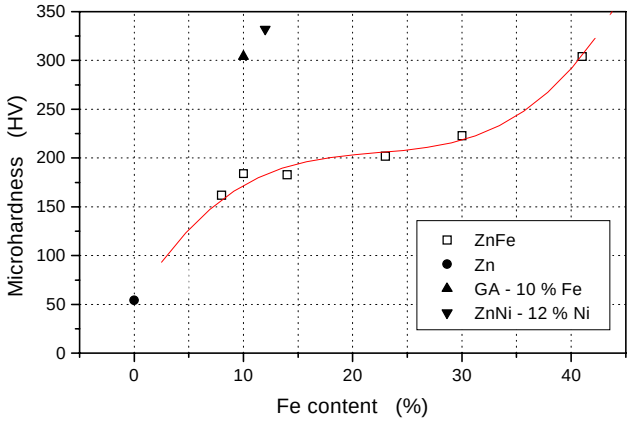

Fig. 4 Microhardness of electroplated zinc-iron coatings in function of the iron content (Zn, electroplated Zn; GA, galvannealed)

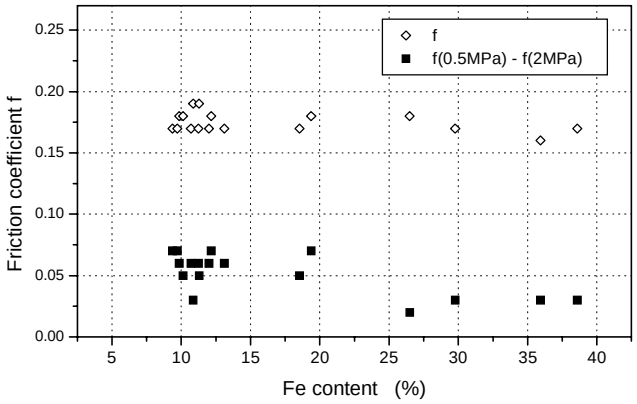

Fig. 5 Influence of the iron content on the friction behavior of electroplated zinc-iron coatings

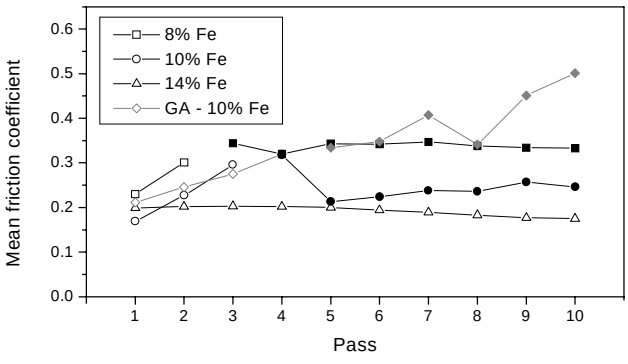

Fig. 6 Comparison of the friction behavior of galvannealed and electroplated zinc-iron layers in the flat die test (GA, galvannealed). Black symbols indicate the presence of stick slip marks.

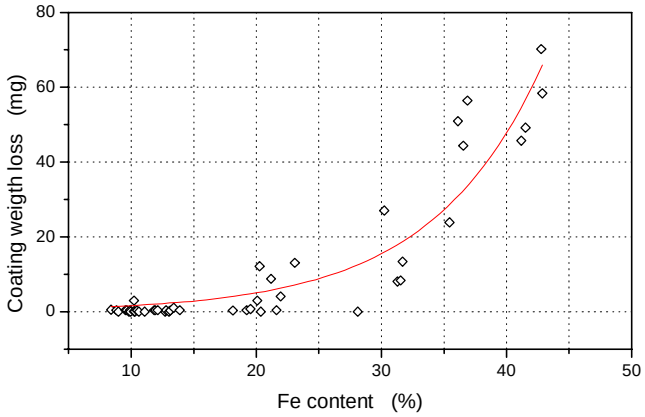

Fig. 7 Influence of the iron content on coating weight loss in a 60° V-bend test

that larger amounts of Γ_1 and Γ phases are detrimental to the formability of the material. Figure 8 shows back scattered electron (BSE) micrographs of the compressed zone after removal of the tape. At low iron contents, stress accommodation results in cracking of the deposited layer. As the Γ_1/Γ fraction in the coating increases the peeling proceeds, and the damaged zone broadens. At 30 wt% Fe the full width of the tape is covered with zinc-iron particles. Residual particles still adhering to the substrate show severe cracking.

The performance of zinc-iron electroplated sheet steel during deep drawing was evaluated by a cup test. For these tests the iron content of the coatings ranged from 8 to 14 wt%. Figure 9 shows coating weight loss and quantity of lubricant of the tested materials. Although the amount of oil picked up by the galvannealed materials exceeds the amount of lubricant in the case of electroplated layers, the coating weight loss for zinc-iron electrocoated sheet steel is comparable to the weight loss for pure zinc coated materials (Ref 30), while the galvannealed materials show a significant increase in powdering rate when the iron content of the coating increases. Moreover, at 10 wt% Fe, the iron content corresponding to commercial galvannealed layers, the amount of powdering for galvannealed material is considerably higher than for the zinc-iron electroplated sheet steel.

Scanning electron microscopy revealed that both galvannealed and zinc-iron layers show significant cracking after deep drawing. Up to 10 wt% Fe, the extent of cracks in zinc-iron layers is comparable to that in galvannealed layers, but in the case of electrodeposited layers the cracks are wider. Above 10 wt% Fe the electrocoated material shows markedly more cracks (Fig. 10). The homogeneous phase distribution over the coating thickness in zinc-iron deposits creates a higher capacity for stress accommodation through cracking than in the case of the layered galvannealed coatings. It should also be noted that for galvannealed coatings the induced cracks in some cases continue in the substrate while with electroplated layers the substrate remains free of cracks (Fig. 11). According to Deits and Matlock (Ref 31), this can be attributed to the effect of galvannealing on the integrity of the ferrite grain boundaries because during the galvanizing process the near-surface ferrite grains are often coated by a thin layer of zinc that has diffused along the grain boundaries.

Figure 10(e) to (g) shows detail of cracks after phosphatation of the zinc-iron coated cups. Although the cracks are still visible after phosphatation, the phosphate crystals seem to cover the cracks.

Unlike galvannealed materials, zinc-iron electroplated material has a lap shear strength, which is not influenced by the type of steel substrate. However, as can be seen from Fig. 12,

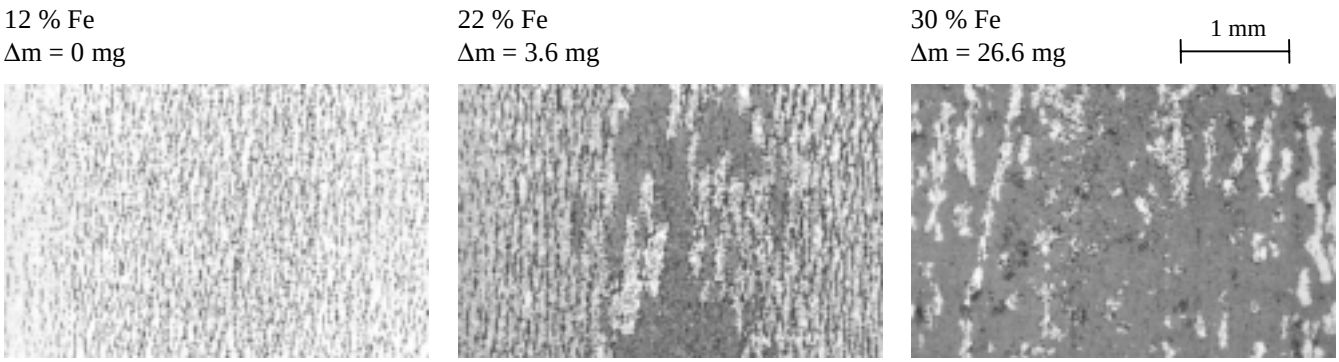

Fig. 8 Scanning electron microscopy images of the coatings after a 60° V-bend test

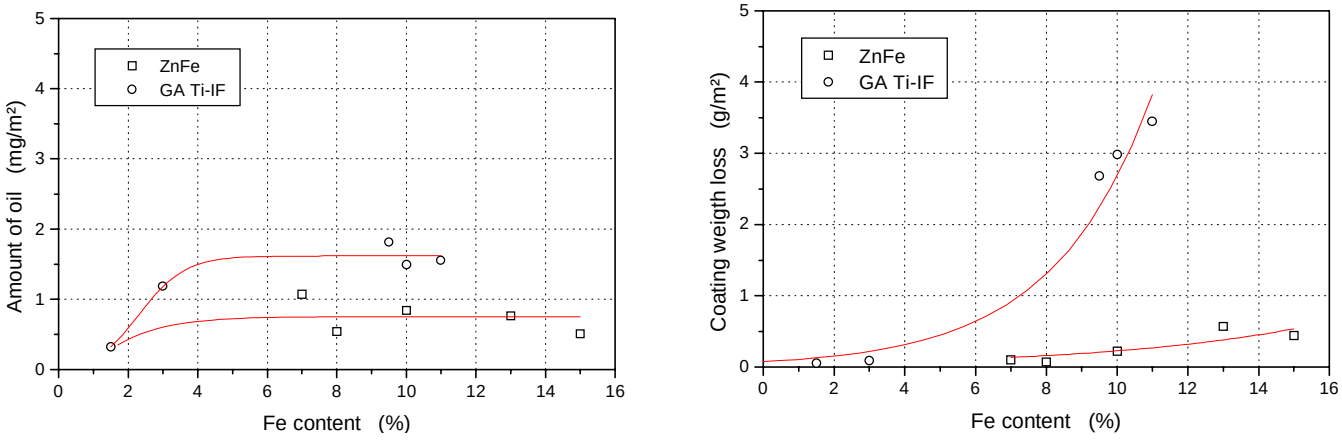

(a) **(b)**

Fig. 9 Influence of the iron content on (a) oil pick-up and (b) coating weight loss in the cup test (ZnFe, electroplated ZnFe; GA, galvannealed)

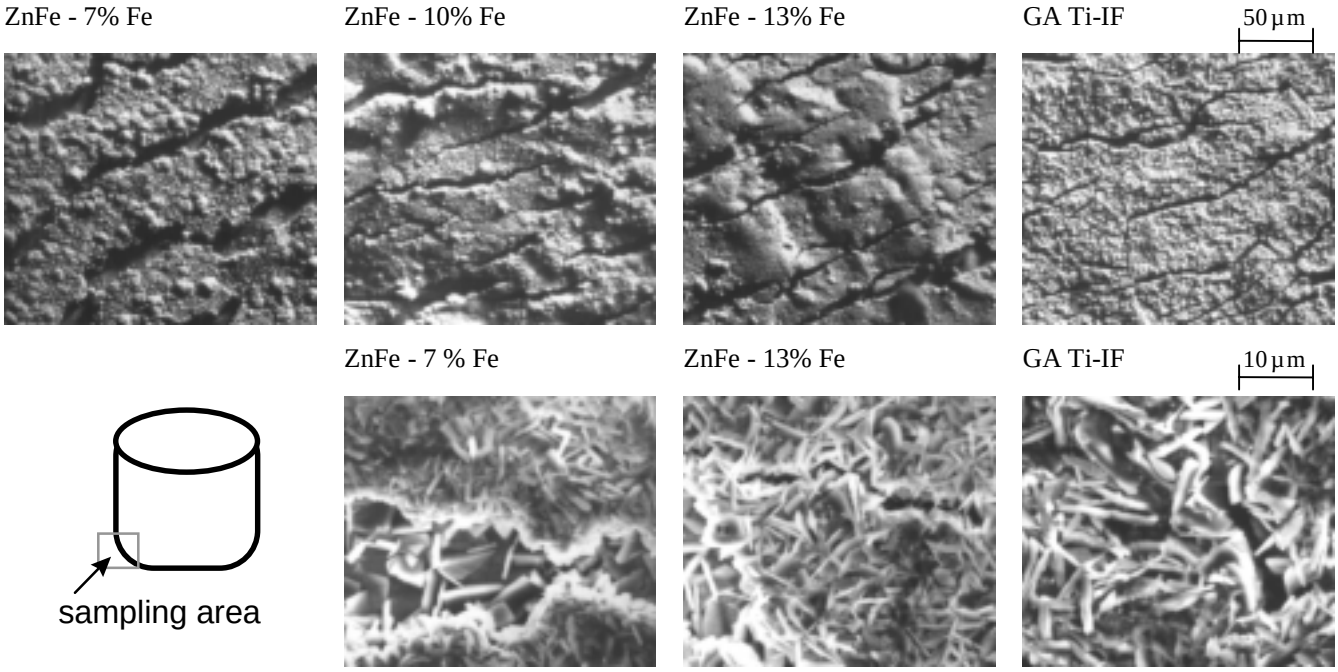

Fig. 10 Scanning electron microscopy images (top row) before and (bottom row) after phosphatation of the deep drawn cups

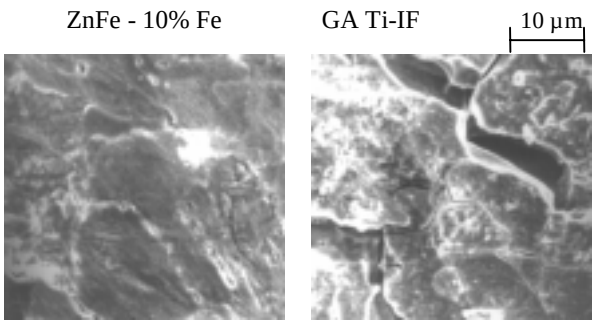

Fig. 11 Detail of the substrate morphology after deep drawing and removal of the coating

the lap shear strength measured on zinc-iron electroplated material with 8 to 14 wt% Fe is comparable with that of DDQ interstitial free (IF) galvannealed samples. An increase in the iron content of the coating lowers the bonding strength, but the influence of iron content is less decisive than in case of galvannealed materials where the zinc-iron phase distribution within the coating strongly influences the adhesion strength (Ref 32). Visual evaluation of the samples showed that while galvannealed material often exhibits a more complex fracture path, over 90% of the fracture plane was situated at the substrate/coating interface in the case of the zinc-iron materials. However, it should be noted that for the electroplated material the pretreatment appeared to be less effective than in an industrial line. Higher lap shear strengths and cohesive fracture, as for zinc and other η-rich materials, is expected for industrial pretreatment. The presence of the ductile η phase is expected to reduce the shear stress intensity at the substrate/coating interface because local plastic deformation will induce stress relaxation (Ref 32, 33).

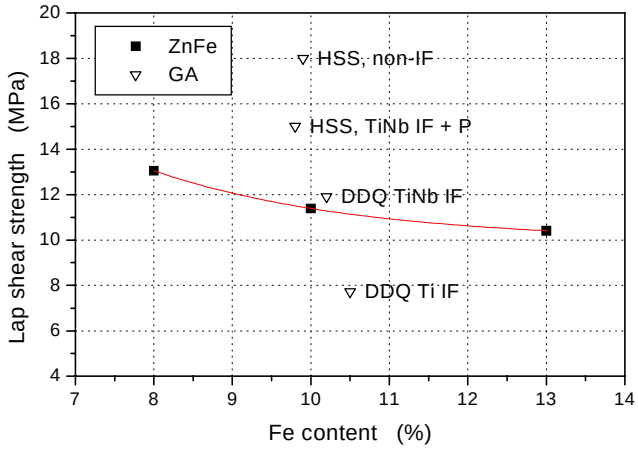

Fig. 12 Influence of the iron content on the lap shear strength of zinc-iron electroplated sheet steel (ZnFe, electroplated ZnFe; GA, galvannealed; HSS, high strength steel; DDQ, deep drawing quality; IF, interstitial free steel)

4. Conclusions

The following conclusions can be drawn:

The relation between phase composition, iron content, and the formability characteristics of zinc-iron electroplated sheet steel has been investigated. Although the soft η phase appears to be the main component in zinc-iron coatings with less than 16 wt% Fe, Γ_1 particles are present even at low iron contents. As the iron content in the coating increases, the Γ_1 fraction increases and the coating becomes harder and more brittle. Whereas a change of iron content in the coating does not significantly affect the friction behavior, the deformation behavior mainly depends on the phase composition of the coating layer:

above 16 wt% Fe the presence of the Γ_1 phase induces substantial powdering and flaking during deformation. At iron contents above 30 wt%, bending of the coated product results in the full delamination of the coating. However, at low iron contents zinc-iron electroplated sheet steel has a superior deformation behavior, and it exhibits a high capacity for stress accommodation through cracking while the adherence of the coating to the substrate is preserved.

References

1. T. Hada, Present and Future Trends of Coated Steel Sheet for Automotive Industry, *Proc. Int. Conf. on Zinc and Zinc Alloy Coated Steel Sheet (GALVATECH)* (Tokyo), ISIJ, 1989, p 111
2. T. Adaniya, Trend of Corrosion Resistant Steels for Automobile Use in Japan, *NKK Tech. Rev.*, (No. 63), 1991, p 1
3. T. Watanabe, M. Ohmura, T. Honma, and T. Adaniya, Iron Zinc Alloy Electroplated Steel for Automotive Body Panels, *SAE Technical Paper Series*, No. 820424, 1982
4. T. Hada, T. Fujiwara, T. Kanamaru, M. Nakayama, and T. Horita, Zinc-Iron Alloy Coated Steel Sheets for Automotive Corrosion Protection, *Proc. Int. Conf. on Surface Modifications and Coatings*, American Society for Metals, 1985, p 29
5. E. Gallo and D.K. Matlock, The Importance of Microstructure on the Formability of Galvannealed IF Sheet Steel, *Proc. Int. Conf. on Zinc and Zinc Alloy Coated Steel Sheet (GALVATECH)* (Chicago), ISIJ, 1995, p 739
6. T. Irie, Development of Zinc-Based Coatings for Automotive Steel Sheet in Japan, *Zinc-Based Steel Coating Systems: Metallurgy and Performance*, The Minerals, Metals and Materials Society/AIME, 1990, p 143
7. T. Kanamaru, M. Nakayama, Y. Ogawa, J. Morita, and K. Arai, Properties of Iron-Zinc Electroplated Galvannealed Steel Sheet, *Nipp. Steel Tech. Rep.*, Vol 63, 1994, p 23
8. K. Kondo, Morphology and Microstructure of Electrodeposited Zinc-Iron Binary Alloys, *ISIJ Int.*, Vol 29, 1989, p 517
9. K. De Wit, J. Dilewijns, A. De Boeck, and B. De Cooman, The Influence of Fe-Content and Phase Composition on the Application Properties of Zinc-Iron Electrodeposited Steel Sheet, *Proc. Int. Conf. on Zinc and Zinc Alloy Coated Steel Sheet (GALVATECH)*, ISIJ, 1995, p 399
10. Y. Liu, Effect of Coating Characteristics on Friction and Formability of Zn-Fe Alloy Electroplated Sheet Steel, *J. Mater. Eng. Perform.*, Aug 1996, p 469
11. H. Kojima, T. Yamamoto, K. Ito, T. Fujiwara, and T. Kanamaru, Properties of Zn-Fe Alloy Electroplated Steel Sheets, *SAE Technical Paper Series*, No. 840214, 1984
12. T. Adaniya, M. Sagiyama, and T. Honma, Phase Composition and Properties of Electrodeposited Zn-Fe Alloy, *Nippon Kokan Tech. Rep.*, (No. 43), 1985, p 33
13. A. De Boeck, L. Vanlerberghe, and M. Vanthournout, Quantitative Analysis of Zinc and Zinc Alloy Coatings on Steel, *La Revue de Métallurgie-CIT*, Oct 1993, p 1277
14. M. Vermeulen, Development of a New Technique to Characterize the Tribological Behaviour of the Steel-Oil-Die System, *Proceedings of the SIBETEX Seminar*, OCAS, Zelzate, 1992
15. W. Warnecke and N. Müschenborn, Formability Aspects of Galvannealed Steel Sheet, *BDDRG Conference Proceedings* (Amsterdam, The Netherlands), May 1985
16. R. Krämer, "Study of Methods for Evaluation of the Powdering and Flaking Behavior of Coated Sheet", thesis, Rheinische Fachhoch-schule Köln, 1992 (in German)
17. J. Hisamoto, K. Ikeda, N. Yamamura, and H. Satoh, The Effect of Coating Hardness on the Peeling-Off Behavior of Electrogalvanized Steel Sheets and Some Aspects of Their Press Formability, *Zinc-Based Steel Coating Systems: Metallurgy and Performance*, The Minerals, Metals and Materials Society/AIME, 1990, p 333
18. J.M. Van der Hoeven, Simulation of Friction and Galling in Drawing Processes, *Proceedings of the SIBETEX Seminar*, OCAS, Zelzate, 1992
19. Y. Yau and S.G. Fountoulakis, Characterization of the Coating-to-Steel Interface Strength in ZnNi Coated Sheet Steel, *Zinc-Based Steel Coating Systems: Metallurgy and Performance*, The Minerals, Metals and Materials Society/AIME, 1990, p 371
20. C. Ortlieb and A. De Boeck, Internal document, OCAS N.V., J. Kennedylaan, 3, B 9060 Zelzate, Belgium, June 1995
21. C.A. Drewien, Phase Transformations in Electrodeposited Iron-Zinc Alloy Coatings, Ph.D. dissertation, Lehigh University, June 1992
22. K. Kondo, S. Hinotani, and Y. Ohmori, Crystal Structure and Morphology of Electrodeposited Zinc-Iron Binary Alloys, *J. Appl. Electrochem.*, Vol 18, 1988, p 154
23. T. Fujieda, A. Naganawa, M. Toyota, S. Higuchi, and S. Takahashi, Structure of Electrodeposited Zn-Fe Alloy in the Zn-Rich Region, *ISIJ Int.*, Vol 32, 1992, p 1044
24. A.S. Koster and J.C. Schoone, Structure of the Cubic Iron-Zinc Phase $Fe_{22}Zn_{78}$, *Acta Cryst.*, Vol 37B, 1981, p 1905
25. D.J. Meuleman, S.G. Denner, and F.L. Cheng, The Effect of Zinc Coatings on the Formability of Automotive Sheet Steels, *SAE Technical Paper Series*, No. 840370, 1984
26. M. Pimminger, F.M. Androsch, and S. Wiesinger, Zinc-Nickel Alloy Electroplated Steel Sheet—Production and Properties, *Conference Proceedings of the Fourth International Zinc Coated Steel Conference* (Paris), 1994, S1F
27. G. Claus, J. Dilewijns, B.C. De Cooman, and U. Meers, Determination of the Process Window for Optimal Galvannealing of Ti-IF Steel, *Proc. Int. Conf. on Zinc and Zinc Alloy Coated Steel Sheet (GALVATECH)*, ISIJ, 1995, p 107
28. G. Claus, J. Dilewijns, H. Storms, J. Scheers, and B.C. De Cooman, Microstructure and Deformation Properties of Galvannealed Coatings on Ti-IF Steels, *La Revue de Métallurgie-CIT*, June 1995, p 805
29. K.P. Imlau, Production and Properties of Electrolytically Deposited ZnFe Alloy Coatings, Forschungsvorhaben der EGKS, April 1991 (in German)
30. A. De Boeck, "Study of Electrodeposited Zinc and Zinc-Nickel on Sheet Steel", Ph.D. thesis, University of Ghent, Belgium, April 1994 (in Dutch)
31. S.H. Deits and D.K. Matlock, Formability of Coated Sheet Steels: An Analysis of Surface Damage Mechanisms, *Zinc-Based Steel Coating Systems: Metallurgy and Performance*, The Minerals, Metals and Materials Society/AIME, 1990, p 297
32. K. Meseure, C. Xhoffer, B.C. De Cooman, I. Hertveldt, and J. Dilewijns, The Shear Strength of Galvannealed Coatings on IF-Steels, *Conference Proceedings of the Fifth International Zinc Coated Steel Conference* (Birmingham), 1997
33. Y. Adachi, M. Arai, and T. Nakamori, *Coating Adhesion and Interface Structure of Galvannealed Steel*, Tetsu-to-Hagané,Vol 80 (No. 3), 1994, p 225 (in Japanese)